Physiology and Molecular Biology of Plants (August 2023) 29(8):1117–1134
https://doi.org/10.1007/s12298-023-01352-2

RESEARCH ARTICLE

Temporal dynamics of endophytic bacterial and fungal communities during spike development in *Piper longum* L.

Sushma Mishra[1] · **Shilpi Sharma**[2]

Received: 27 February 2023 / Revised: 24 August 2023 / Accepted: 28 August 2023 / Published online: 12 September 2023

Abstract

The female spikes (fruits) of *Piper longum* are widely used in Ayurvedic, Siddha and Unani medicine systems to treat respiratory and digestive disorders. The spikes are rich in piperine, a pharmacologically active amide alkaloid and a potent bioavailability enhancer, which accumulates to the highest level during the dark-green stage of spike development. Plant-associated microbiota influence the plant's fitness, response, and production of economically important metabolites. Considering the economic importance of piperine and other spike-derived alkaloids, understanding microbial community dynamics during spike development would be key to bioprospecting for economically important metabolites. In the present study, the structural diversity of microbial communities associated with early (SI), mid (SII), and late (SIII) stages of spike development in *P. longum* has been analysed by Illumina-based amplicon sequencing of 16S rRNA gene and ITS region. Results revealed that spike development significantly drives the diversity and abundance of spike-associated microbiota, especially bacterial communities. *Cyanobacteria* and *Ascomycota* constituted the most abundant bacterial and fungal phyla, respectively, across all stages of spike development. Interestingly, *Halomonas, Kushneria* and *Haererehalobacter* were found to be exclusively associated with SIII (corresponding to economically important) stage of spike development. *Sphingomonas, Mortierella, Cladosporium* and *Vishniacozyma* constituted the core microbiome of the spike. Besides, PICRUSt analysis revealed that amino acid metabolism was the most dominant metabolic function attributed to spike-associated bacterial communities. To the best of our knowledge, this is the first study to investigate the endomicrobiome dynamics during spike development in a medicinal plant species.

Keywords Spike · Plant development · Microbiome · Amplicon sequencing · Medicinal plant · *Piper longum*

Introduction

Our understanding of the role of the microbiome in plant responses has remarkably increased in the past few decades. The plant endosphere is known to be predominantly inhabited by bacterial and fungal communities, which fine-tune the overall plant health and fitness (Mishra et al. 2021a). Most studies investigating the influence of plant development on microbiome structure have focussed on the rhizosphere microbiome. One such study, assessed the impact of plant development on microbial community structure during the young seedling, adult stage, flowering and senescence in pea, wheat and sugarbeet (Houlden et al. 2008). Using a combination of culture-dependent approach and denaturing gradient gel electrophoresis, the authors concluded that while the rhizospheric bacterial and fungal community structure was more or less stable in pea and wheat, dynamic shifts were observed in sugarbeet rhizosphere during its life cycle. Further, the role of plants in selecting specific microbial communities, especially during the mature plant stage (*vs*. seedling stage) was also recorded. Chaparro et al. (2014) studied the rhizosphere microbiome at seedling, vegetative, bolting, and flowering stages in *Arabidopsis*. They reported that plants at particular stages of development selectively recruit a subset of microbiota to assist or suit specific plant functions.

✉ Sushma Mishra
mishra_sushma@lkouniv.ac.in

✉ Shilpi Sharma
shilpi@dbeb.iitd.ac.in

[1] Department of Botany, University of Lucknow, Lucknow, Uttar Pradesh 226007, India

[2] Department of Biochemical Engineering and Biotechnology, Indian Institute of Technology Delhi, New Delhi, Delhi 110016, India

Piper longum is widely used in Ayurvedic, Siddha and Unani medicine systems. It is a dioecious species, with unisexual flowers borne in spikes on separate male and female plants (Babu et al. 2006). The female flowers of *P. longum* are yellow or creamy white in colour, and are borne in spikes. The mature fruit is a black-coloured drupe, of ~ 2–3 cm in length (Kanimozhi and Sujatha 2015; Gajurel et al. 2021). The female spikes (commonly known as *pippali* in the trade of commerce) are shorter (~ 2–3 cm long) than the male spikes (6–7 cm long), and are rich in piperine, piperlongumine and other bioactive compounds (Rajopadhye et al. 2012; Kanimozhi and Sujatha 2015). Hence, female spikes are in great demand for use in more than 100 Ayurvedic formulations to treat respiratory and digestive disorders. Further, piperine is considered to be the most potent bioenhancer, with reports showing 30–200% increase in bioavailability of different classes of drugs (Atal and Bedi 2010). Also, female spikes are widely used as a spice for seasoning dishes. According to National Medicinal Plant Board, *P. longum* is a high-volume trade plant in the Indian market (Ved and Goraya 2008; NMPB).

Our previous studies have reported the endophytic microbial diversity in *P. longum* using both culture-dependent and culture-independent approaches (Mintoo et al. 2019; Mishra et al. 2021b). Spikes were found to harbour specific microbial communities with the potential to produce bioactive compounds including piperine (Mishra et al. 2021b). Besides, recently the growth promoting effects of *P. longum* bacterial endophytes on seed germination and early seedling development in wheat and maize have also been reported (Phurailatpam et al. 2022). Therefore, considering the demand of *P. longum* worldwide, and the prevailing role of the microbiome in affecting plant health and responses, the study aims to assess the temporal dynamics in microbiota abundance and composition with respect to the stage of spike development (Supplementary Fig. S1).

Materials and methods

Sampling

The female spikes of *P. longum* at three different stages of development (SI, SII, and SIII) were harvested from healthy, female plants of *P. longum*. Stage SI represents spikes < 1 cm in length, SII represents spikes with a length of 1–2 cm, and SIII represents spikes > 2 cm in length (Supplementary Fig. S1). Three biological replicates for each stage were collected from asymptomatic plants maintained in University of Lucknow, Lucknow (26.8633° N, 80.9360° E).

Surface sterilization and genomic DNA isolation from spikes

The spike samples were surface-sterilized by washing in running tap water, followed by immersing in 70% ethanol and 4% sodium hypochlorite for 5 s and 90 s, respectively, and finally rinsing in sterile distilled water (Suryanarayanan et al. 1998). Next, genomic DNA was isolated from surface-sterilized plant samples using QIAGEN's DNeasy PowerSoil Pro kits. The samples with 260/280 values of ~ 1.8 to 2 (as checked by small volume spectrophotometer), were processed for PCR amplification.

PCR amplification of 16S rRNA gene and ITS region

Approximately 40 ng of the extracted DNA was used as a template for the amplification of V3-V4 region of 16S rRNA gene using 357F and 806R primers (Klindworth et al. 2013). For amplification of ITS region of fungal rRNA, the ITS1 forward and ITS2 reverse primers were used (White et al. 1990). The PCR conditions used for amplification of both 16S and ITS amplicons were an initial denaturation of 95 °C for 3 min, followed by 25 cycles of denaturation at 95 °C for 15 s, primer annealing at 60 °C for 15 s, and extension at 72 °C for 30 s, and a final extension at 72 °C for 10 min and hold at 4 °C. PCR products were checked on 1.2% agarose gel and a quality check was done with a small-volume spectrophotometer.

The subsequent steps including preparation of 16S rRNA and ITS amplicon libraries, quality check and sequencing of libraries was performed following the protocol of Mishra et al. (2021b). The 16S rRNA gene and ITS region sequencing reads have been submitted to the Sequence Read Archive of the National Centre for Biotechnology Information under the Bioproject number, PRJNA860932 and PRJNA869034, respectively.

Data processing

The 16S rRNA and ITS sequencing data were processed using QIIME 2 microbiome analysis tool (Bolyen et al. 2019). The data were filtered for low-quality sequences by applying the low count (prevalence level 20% for minimum count 4) and low variance (inter-quartile range of 10%) filters. Next, the variability in sampling and sequencing depth was addressed by rarefying the data to the minimum library size and lowest sequencing depth. KRAKEN 2, the taxonomic classification system was used for OTU calling at a

cut-off of 0.97 (Wood et al. 2019). A representative sequence from each OTU was selected, followed by its taxonomic assignment using GreenGenes database for 16S rRNA gene sequences and UNITE for ITS sequences. The alpha diversity analysis was performed by Chao1, Shannon, Simpson and Fisher using the ANOVA statistical test. Beta diversity analysis was performed using Bray–Curtis index distance method based on Permutational MANOVA (PERMANOVA) statistical method. The heatmaps were constructed at the genus level using Ward cluster algorithm based on Euclidean distance measure.

Advanced analysis

The correlation network between microbial communities was built using SparCC (Sparse Correlations for Compositional data) algorithm at a p-value of 0.05. The red lines indicate a positive correlation, while the blue indicate a negative correlation between the taxa pairs. Further, Kruskal–Wallis rank sum test was performed to detect features with significant differential abundance with regards to class labels, followed by Linear Discriminant Analysis to evaluate the relevance or effect size of differentially abundant features. The data were analyzed with the p-value cut-off of 0.1 with FRD-adjusted filter and Log LDA score of 2.0.

The potential metabolic functions of bacterial communities associated with spike development were obtained by Phylogenetic Investigation of Communities by Reconstruction of Unobserved States (PICRUSt) analysis (Langille et al. 2013). The potential trophic modes and functional guilds were predicted for fungal communities using the FUNGuild (https://github.com/UMNFuN/FUNGuild) database (Nguyen et al. 2016). The core microbiota analysis was performed by selecting the bacterial and fungal taxa present at a sample prevalence of 20% and relative abundance of 0.1%.

Results

The medicinal plant *P. longum* shows a staggered or non-synchronous flowering pattern. The spikes take around two months to mature from the time of emergence (Gajurel et al. 2021; *Piper longum*—Vikaspedia). Therefore, at any time point during the flowering season, spikes at different stages of spike development could be seen (Supplementary Figure 1). Commercially, the female spikes are picked at blackish green stage (i.e., fully mature but unripe), when they are most pungent due to highest concentration of piperine (Joshi et al. 2013; Khound et al. 2019). This is because the piperine content of fruits increases with maturity, from ~ 0.53% (at 14–16 days) to ~ 0.9% (at 40–45 days), after which the "quality" (in trade terminology) is said to decline (Babu et al. 2006).

In the present study, for targeted amplicon sequencing of spike-associated microbial communities, bacterial 16S rRNA gene and fungal ITS region were amplified from nine spike samples representing three replicates of each of the three stages (SI, SII, SIII) of spike development in *P. longum*. A total of 22,55,270 and 14,47,434 high-quality reads were generated in 16S rRNA gene and ITS amplicon libraries, respectively. Thereafter, 16S rRNA sequencing reads were clustered into an average of 124,163.125 OTUs, and ITS sequencing reads were clustered into an average of 30,459.1 OTUs at 97% sequence similarity (Supplementary Tables 1, 2). The alpha diversity analyses for 16S rRNA gene and ITS sequences have been represented in Supplementary Figure 2 and 3, respectively. The alpha diversity analysis reveals the number of taxa or relative abundance of taxa within the sample. The alpha diversity analyses revealed that SIII stage distinctly harbors the most abundant and diverse bacterial communities, followed by SII, and least at the SI stage of spike development (Supplementary Figure 2). Similarly, the diversity of fungal communities was highest at SIII stage, while the SI and SII stages showed equivalent values (Supplementary Figure 3). Next, beta diversity analysis was performed to determine how similar or dissimilar the microbial communities are between different samples (here, different stages of spike development). The results of beta diversity analysis showed that the bacterial communities of all the replicates of the SI stage form one group, distinct and away from the replicates of SII and SIII stages (Supplementary Figure 4A). There was much more variation in fungal communities among the replicates across the three stages of spike development (Supplementary Figure 4B).

The rarefaction curves representing species richness for a given sample size for 16S rRNA gene and ITS segment amplicon sequencing have been represented in Supplementary Figure 5. A fair representation of microbial communities (i.e., both abundant and rare species) in the samples could be inferred from the plateau-like phase seen in the rarefaction curves for both 16S rRNA gene and ITS amplicon sequencing (Supplementary Figure 5A and B).

Taxonomy plot analysis of bacterial and fungal communities across spike development stages

To study the dynamics of plant-associated microbial communities during spike development, the average relative abundance of bacterial and fungal communities across different stages of development (SI, SII and SIII stages) was studied. The 16S rRNA amplicon analysis revealed that *Cyanobacteria* were the most dominant (constituting > 80%) phylum across all the stages of spike development, followed by *Proteobacteria*. The abundance of *Bacteroidetes* and *Firmicutes*

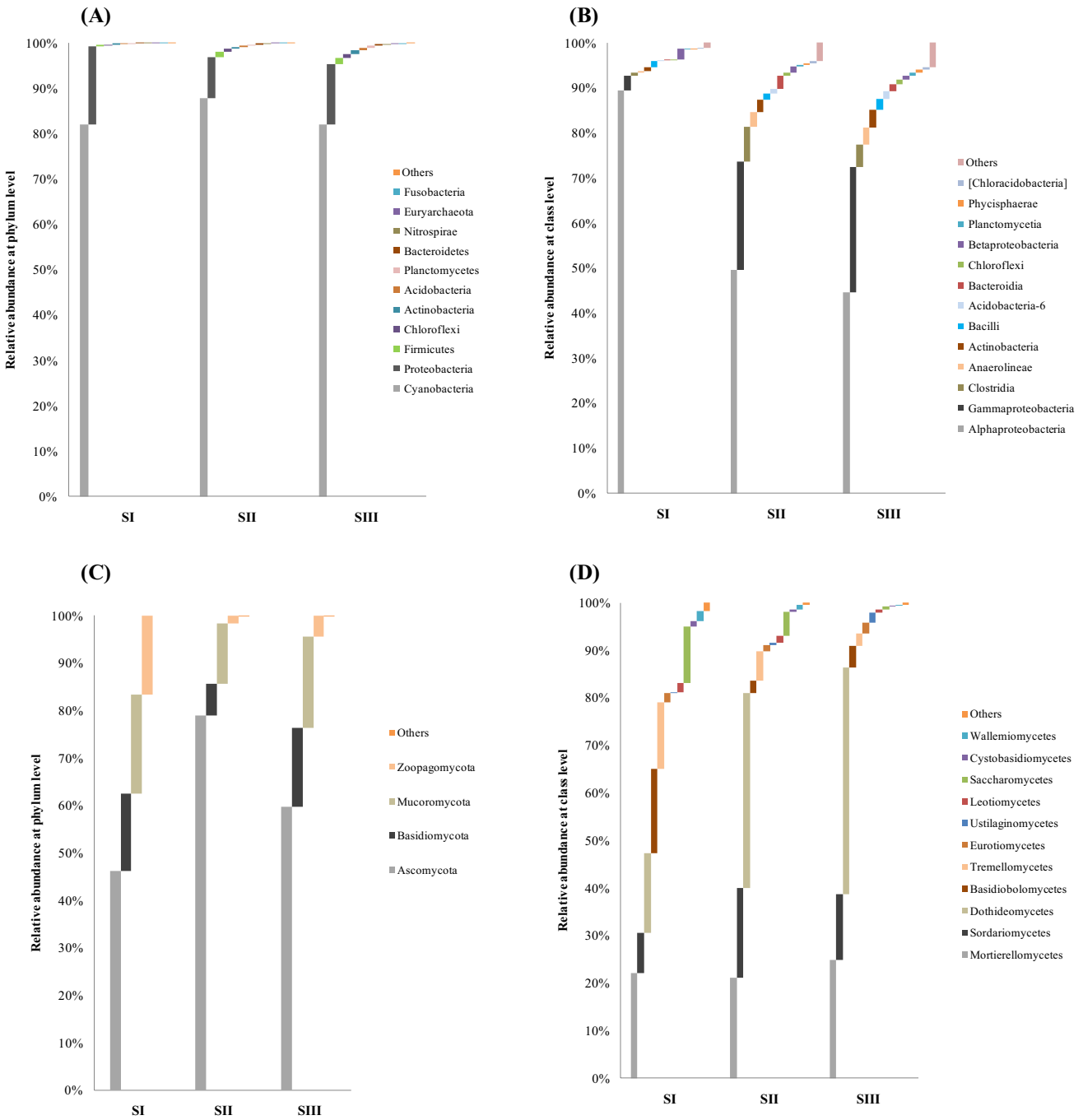

Fig. 1 Relative abundance (in percentage) of microbial communities during spike development: Bacterial taxa at phylum (**A**) and class (**B**) levels; fungal taxa at phylum (**C**) and class (**D**) levels. The number of OTUs on Y-axis represents the average of three replicates for each of the three stages: early (SI), mid (SII), and late (SIII) stages of spike development in *P. longum*

phyla increased during mid-to-later stages of spike development. Interestingly, the abundance of several phyla, such as *Planctomyces, Actinobacteria, Acidobacteria* and *Chloroflexi*, was highest during the SIII (late) stage of spike development (Fig. 1A). Further, a similar trend was observed at the class level, where *Clostridia*, *Anaerolineae, Actinobacteria, Bacilli* and *Acidobacteria-6* were the most abundant during the SIII stage of spike development (Fig. 1B). At the genera level, the most abundant taxa during early stage (SI) of spike development included *Sphingomonas, Herbaspirillum, Sphingobacterium* and *Corynebacterium* (Fig. 2A). The mid stage (SII) of spike development was marked by an increased abundance of *Bifidobacterium, T78, Pseudomonas, Prevotella, Bacteroides, Faecalibacterium,*

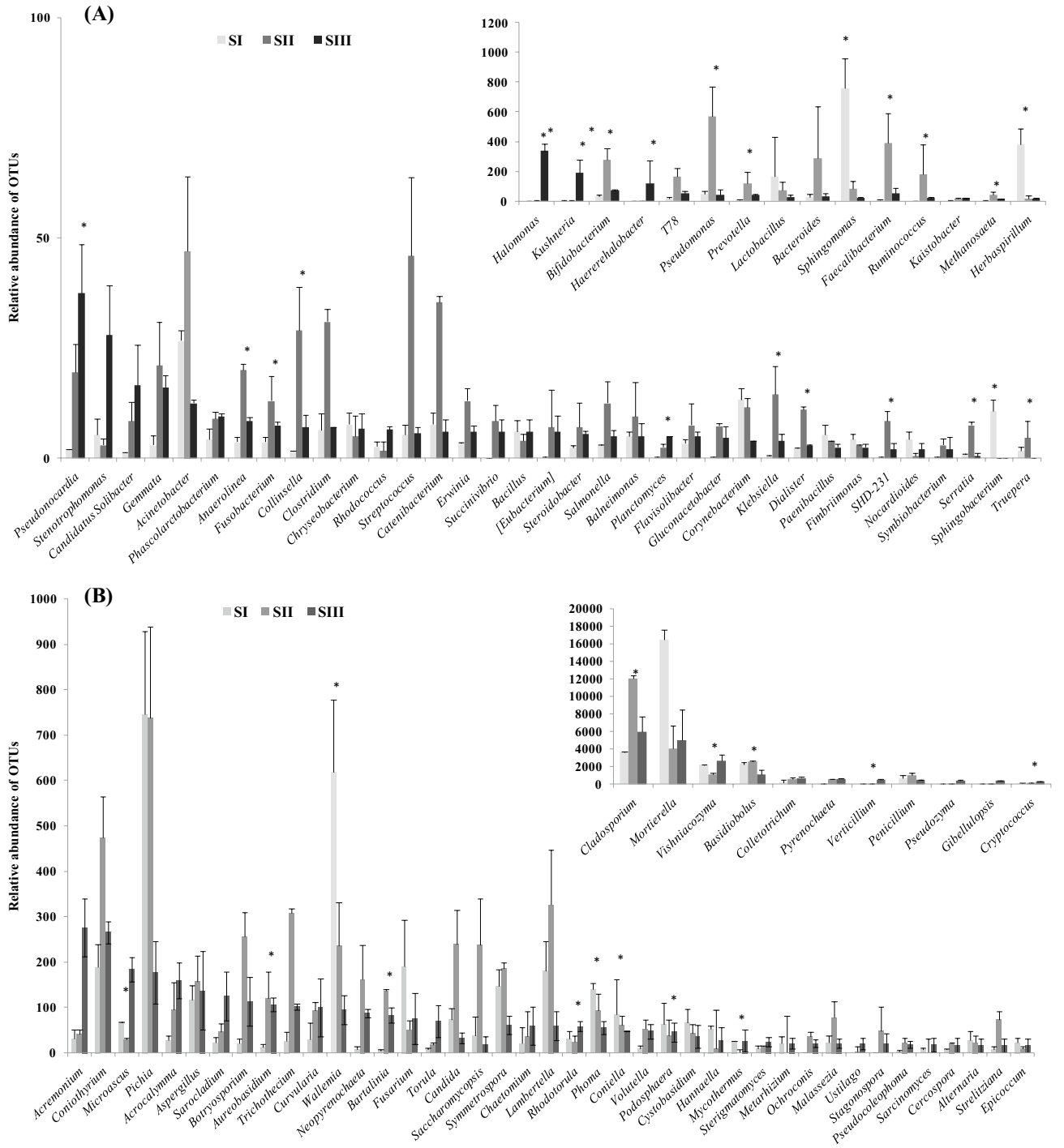

Fig. 2 Relative abundance of bacterial (**A**) and fungal (**B**) genera during early (SI), mid (SII), and late (SIII) stages of spike development. The inset figures show the taxa with abundance higher than the main graph. Bars represent the mean and error bars show standard error ($n = 3$). Statistical significance was calculated by Kruskal Waalis test with Benjamini–Hochberg correction at significance level $p \leq 0.05$ (denoted by *)

Ruminococcus, Methanosaeta, *Acinetobacter, Anaerolinea, Fusobacterium, Collinsella, Clostridium, Streptococcus, Catenibacterium, Erwinia, Succinivibrio, Salmonella, Balneimonas, Klebsiella, Dialister, SHD-231, Serratia* and *Truepera*. The bacterial genera abundant during the late stage (SIII) were *Halomonas, Kushneria* and *Haererehalobacter*; these were almost absent from the previous stages of spike development. The other genera that were the most

abundant during SIII stage included *Pseudonocardia, Stenotrophomonas, Candidatus Solibacter, Rhodococcus* and *Planctomyces* (Fig. 2A).

The fungal microbiome associated with different stages of spike development was studied by ITS amplicon sequencing, which revealed that *Ascomycota* was the most abundant phylum, followed by *Mucoromycota* and *Basidiomycota* (Fig. 1C). The phylum *Zoopagomycota* was abundant during early stage (SI) but declined during mid and late stages of spike development. Further, the fungal communities belonging to class *Basidiobolomycetes, Tremellomycetes, Saccharomycetes, Cystobasidiomycetes* and *Wallemiomycetes* were the most abundant during the early stage of spike development; the relative abundance of these taxa was found to decline during later stages of spike development (Fig. 1D). On the other hand, the classes *Sordariomycetes* and *Ustilaginomycetes* drastically increased in abundance in SIII stage of development. In the mid-stage of spike development, *Dothideomycetes* constituted the most abundant (> 60%) class. The most abundant genera during early spike development included *Mortierella, Wallemia, Fusarium* and *Phoma*. Some fungal genera such as *Trichothecium, Coniothyrium, Botryosporium, Candida, Saccharomycopsis, Lambertella, Malassezia, Ochroconis* and *Strelitziana* were specifically abundant during the mid-stage of spike development. Interestingly, the fungal genera *Colletotrichum*, *Pyrenochaeta, Verticillium, Pseudozyma, Gibellulopsis, Cryptococcus, Acremonium, Microascus, Acrocalymma*, *Sarocladium, Torula, Chaetomium* and *Sterigmatomyces* increased in abundance from SI to SIII stages (Fig. 2B).

Comparative abundance of bacterial and fungal genera during spike development

In the heat maps (Fig. 3A and B), each row represents a bacterial/fungal community, and the columns represent average (from three replicates of each stage) OTU abundance during each spike development stage. The high abundance of genera has been indicated by red colour, while low abundance is represented by green colour.

As evident from the heat map shown in Fig. 3A, there was a remarkable shift in the abundance of fungal taxa during spike development. The fungal genera showing the highest abundance at the SI stage included *Cystobasidium, Phaeosphaeria, Starmerella, Calonectria, Microdochium, Geotrichum, Trichoderma, Eutypella, Wallemia, Vishniacozyma, Lambertella, Neophysalospora, Ophiocordyceps, Pichia, Taphrina, Madurella, Plectosphaera, Naganishia, Basidiobolus, Hannaella, Phoma, Epicoccum, Pseudocercospora, Lepidosphaeria, Lophiostoma, Coniella, Latorua, Podospora* and *Rhodotorula*. Likewise, the SII stage was marked by predominant genera such as *Toxicocladosporium, Bullera, Nigrospora, Candida, Melanodothis, Aureobasidium, Medicopsis, Stagonospora, Pyrenochaeta, Strelitziana, Acrocalymma, Bartalinia, Saccharomycopsis, Cladosporium, Coniothyrium, Neopyrenochaeta, Ochroconis, Botryosporium, Pseudocoleophoma* and *Trichothecium*. During SIII stage, the economically important stage of spike development, the most abundant fungal members included *Acremonium, Gibellulopsis, Torula, Chaetomella, Monocillium, Sarocladium, Curvularia, Eupenidiella, Chaetomium, Fusarium, Pseudozyma, Microascus, Sterigmatomyces, Aspergillus, Verticillium, Sarcinomyces, Gliomastix, Rhexothecium, Metarhizium, Podosphaera, Malassezia, Mortierella, Gliocladiopsis, Penicillium, Cercospora, Dendryphiella* and *Volutella*. Interestingly, the abundance level of some fungal genera such as *Alternaria, Symmetrospora, Colletotrichum* and *Cryptococcus*, increased with spike maturity (Fig. 3A). The early (SI) stage of spike development was marked by an increased abundance of bacterial members such as *Methylobacterium, Corynebacterium, Sphingomonas, Herbaspirillum, Kineococccus, Agrobacterium, Sediminibacterium, Deinococcus*, *Acinetobacter* and *Catenibacterium* (Fig. 3B); their levels declined during SII and SIII stages. On the other hand, a higher number of bacterial taxa were found to increase in abundance during the later stages (SII and SIII) of spike development. These include *Faecalibacterium, Ruminococcus, Devosia, Virgisporangium, Gluconacetobacter, Prevotella_1, Succinovibrio, Candidatus_Solibacter, Gemmata, Methanosaeta, Mycobacterium, Erwinia, SHD_231, Dialister, T78, Steroidobacter, Klebsiella* and *Methanobrevibacter.* The bacterial genera that showed the highest abundance during the SIII stage included *Azospirillum, Rhodococcus, Pseudomonas, Stenotrophomonas, Pseudonocardia, Fusobacterium, Kaistobacter, Chloronema, Phascolarctobacterium, Eubacterium, vadinCA02, Planctomyces, Bacteroides, Lactobacillus* and *Symbiobacterium.* Only five bacterial genera, namely *Streptomyces, Clostridium, Prevotella, Serratia* and *Trabulsiella*, showed the highest abundance during the SII stage of spike development (Fig. 3B).

Most abundant genera during each stage of spike development

The ten most abundant bacterial genera during early spike (SI) development were *Sphingomonas, Herbaspirillum, Lactobacillus, Streptomyces, Pseudomonas, Bifidobacterium, Acinetobacter, Methylobacterium, Bacteroides* and *T78* (Fig. 4A-i). Similarly, the ten most abundant bacterial genera during mid-spike (SII) development were *Methylobacterium, Bifidobacterium, Mycobacterium, Pseudomonas, Sediminibacterium, Acinetobacter, Bacterioides, Enhydrobacter, Corynebacterium and Dechloromonas* (Fig. 4A-ii). The late spike (SIII) development stage showed high abundance of *Herbaspirillum, Lactobacillus, Streptomyces, Pseudomonas,*

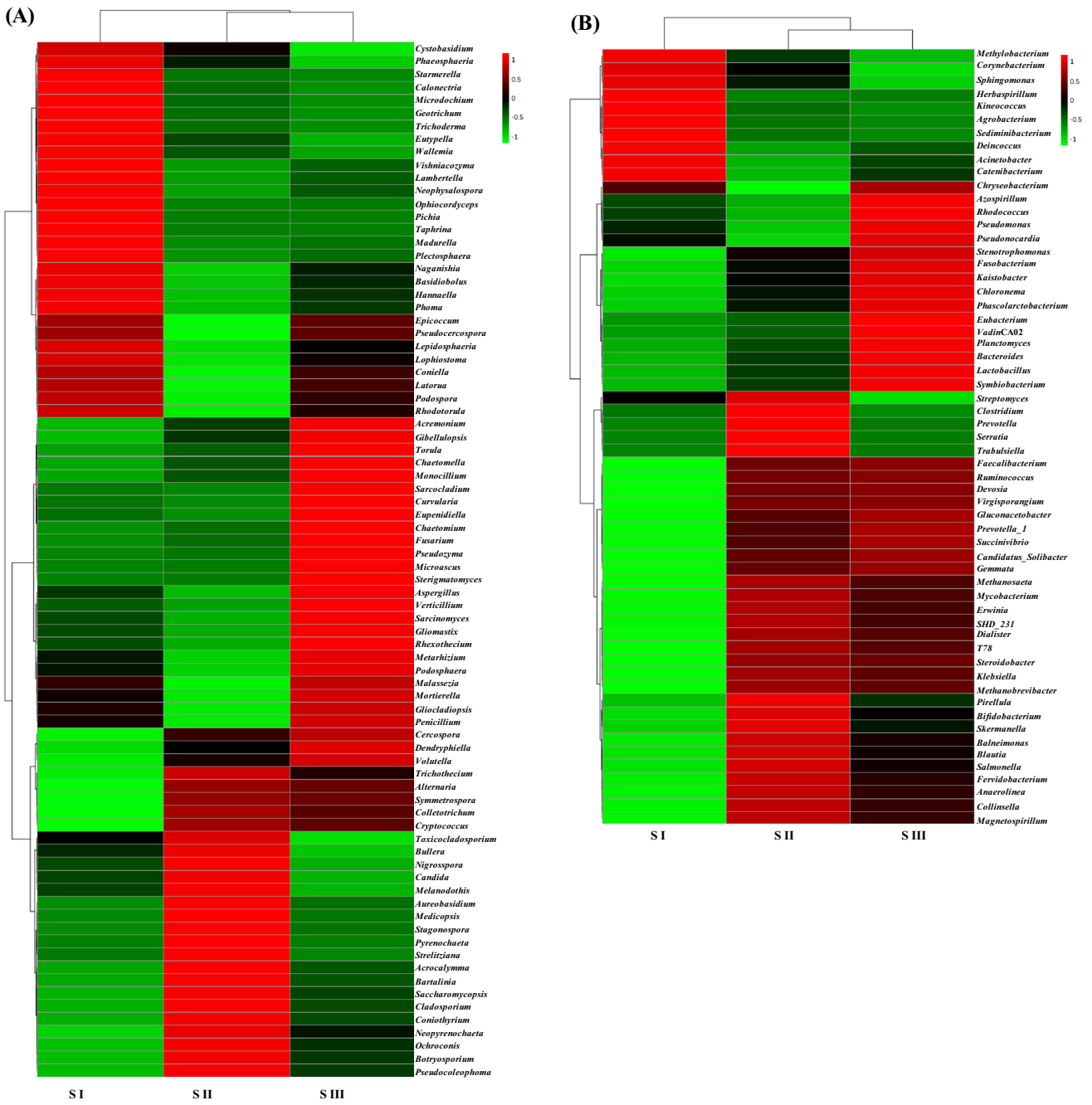

Fig. 3 Heatmaps showing average relative abundance of fungal (**A**) and bacterial (**B**) genera during early (SI), mid (SII), and late (SIII) stages of spike development. Red and green colours represent increase and decrease, respectively, in the OTU abundance during each stage. The heatmaps were constructed at the genus level using Ward cluster algorithm based on Euclidean distance measurements

Bifidobacterium, Acinetobacter, Methylobacterium, Bacteroides, T78 and *Mycobacterium* (Fig. 4A-iii).

Strikingly, there was conservation in the most abundant fungal genera during spike development. For example, *Mortierella, Cladosporium, Basidiobolus, Vishniacozyma, Pichia, Penicillium, Wallemia, Coniothyrium, Lambertella* and *Colletotrichum* constituted the top ten abundant fungal genera during early spike (SI) development (Fig. 4B-i). Similarly, the ten most abundant fungal genera during mid-spike (SII) development were *Mortierella, Cladosporium, Basidiobolus, Penicillium, Pichia, Coniella, Phoma, Vishniacozyma, Hannaella* and *Podosphaera* (Fig. 4B-ii). The late spike (SIII) development stage showed a high abundance of *Mortierella, Cladosporium, Vishniacozyma, Pichia, Fusarium, Basidiobolus, Coniothyrium, Aspergillus, Phoma* and *Microascus* (Fig. 4C-iii).

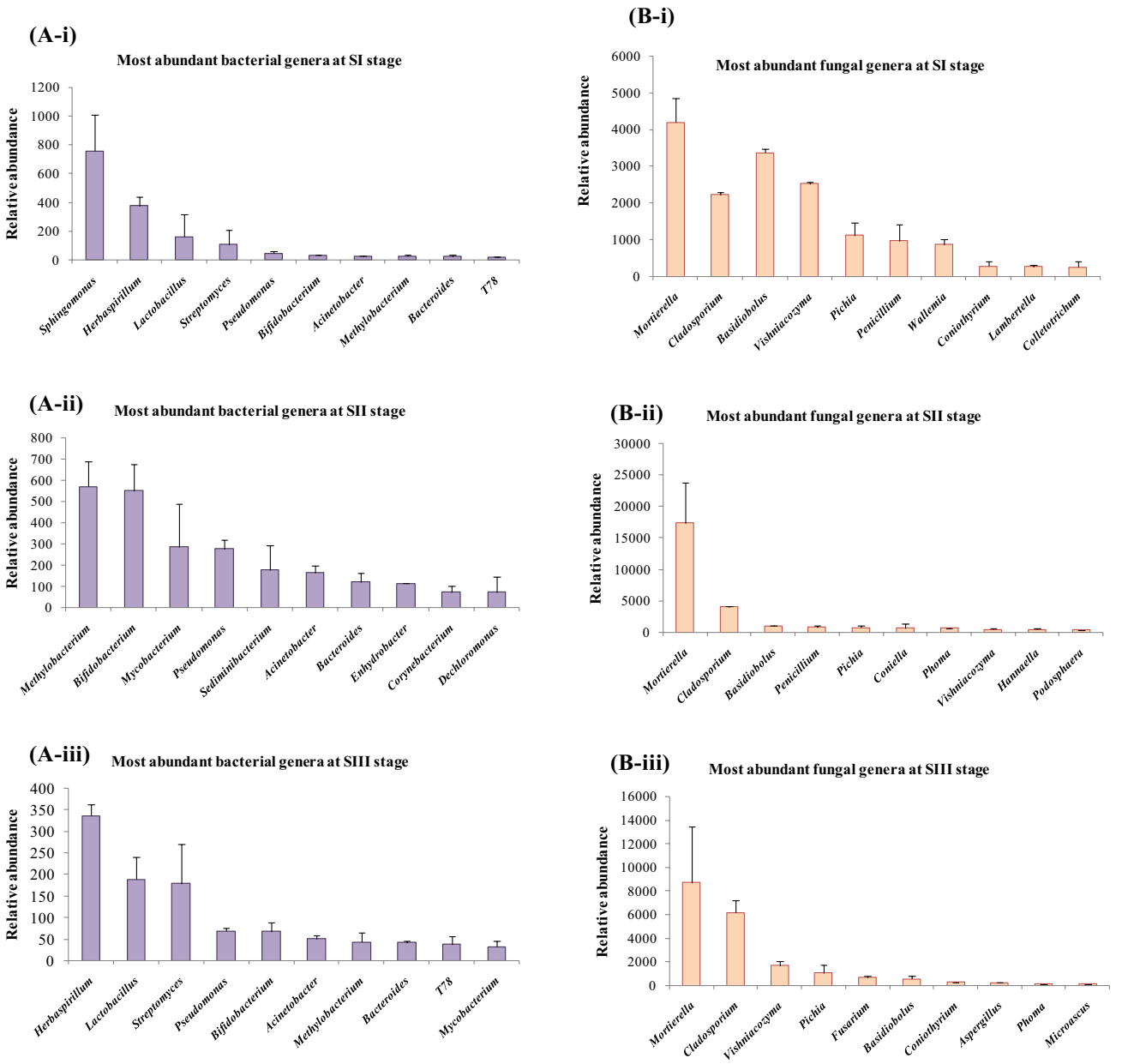

Fig. 4 Ten most abundant bacterial (**A**) and fungal (**B**) genera during early (SI), mid (SII), and late (SIII) stages of spike development. The unclassified/unknown reads were not considered. Bars represent the mean and error bars show standard error ($n = 3$)

Microbial communities common and unique to each spike development stage

The Venn diagrams show that 20, 61, and 23 bacterial genera (Supplementary Figure 6A) and 18, 10, and 26 fungal genera (Supplementary Figure 6B) were unique to SI, SII, and SIII stages, respectively. The microbial communities unique to each stage, and those common to all the stages, have been presented in Tables 1 and 2.

Further, some of these core bacterial and fungal communities underwent remarkable changes in their abundance during different stages, as evident from the heat maps (Fig. 3). The results of core microbiome analysis carried out at a sample prevalence of 20% and relative abundance of 0.1% have been shown in Fig. 5. The core microbial communities of the spike at a prevalence value of 1 included *Sphingomonas, Mortierella, Cladosporium* and *Vishniacozyma* (Fig. 5A and B).

Table 1 Microbial genera unique to each stage of spike development

Early (SI) stage		Mid (SII) stage		Late (SIII) stage	
Bacterial	Fungal	Bacterial	Fungal	Bacterial	Fungal
Actinopolymorpha	*Acanthotrema*	*Acholeplasma*	*Blastobotrys*	*4–1929*	*Anthracocystis*
Asteroleplasma	*Allomyces*	*Acidaminococcus*	*Conioscypha*	*Afifella*	*Ceratobasidium*
Asticcacaulis	*Apiotrichum*	*Actinobacillus*	*Cutaneotrichosporon*	*Alkaliphilus*	*Cercosporella*
BF311	*Ascobolus*	*Actinocorallia*	*Dicyma*	*Arthrobacter*	*Coriolopsis*
Bosea	*Clonostachys*	*Actinomyces*	*Meira*	*Azohydromonas*	*Ctenomyces*
Candidatus Cardinium	*Cordana*	*Aeromicrobium*	*Neophaeosphaeria*	*Brevibacterium*	*Exserohilum*
Cellvibrio	*Fusoidiella*	*Alloiococcus*	*Rachicladosporium*	*C1_B004*	*Heterochaete*
Dokdonella	*Humicola*	*Anabaena*	*Saitozyma*	*CF231*	*Hyalotiella*
Gracilibacter	*Lasiodiplodia*	*Aquicella*	*Ustilago*	*Isosphaera*	*Hypoxylon*
Gramella	*Phialophora*	*Arsenicicoccus*	*Wojnowicia*	*Methanobacterium*	*Italiomyces*
Haliscomenobacter	*Preussia*	*Arthronema*		*Nonomuraea*	*Kernia*
Methylibium	*Pyricularia*	*BD2-6*		*Paracoccus*	*Lectera*
Microbacterium	*Rhodosporidiobolus*	*Blvii28*		*PD-UASB-13*	*Leptoxyphium*
Propionibacterium	*Sonoraphlyctis*	*Brevundimonas*		*Perlucidibaca*	*Malaysiasca*
SC103	*Westerdykella*	*Campylobacter*		*Pilimelia*	*Musicillium*
Shimazuella	*Xeromyces*	*Candidatus Entoth-eonella*		*Planktothricoides*	*Mycothermus*
Sphingobacterium	*Zopfiella*	*Candidatus Xiphin-ematobacter*		*Pseudochrobactrum*	*Papiliotrema*
Sulfuricurvum	*Zymoseptoria*	*Crocinitomix*		*Psychrobacter*	*Parengyodontium*
Ureibacillus		*Cupriavidus*		*RFN20*	*Pseudoacrodictys*
YRC22		*Dechloromonas*		*Slackia*	*Rhinocladiella*
		Desulfobacca		*Sporomusa*	*Sporobolomyces*
		Desulfococcus		*Sulfurospirillum*	*Thyridariella*
		Desulforhopalus		*Syntrophobacter*	*Ustilaginoidea*
		Desulfosarcina			*Verruconis*
		Fusibacter			*Zeloasperisporium*
		HTCC2207			*Zygosporium*
		Hyphomicrobium			
		Kosmotoga			
		Kribbella			
		Lachnospira			
		Lautropia			
		LCP-26			
		Leuconostoc			
		Microcoleus			
		Neisseria			
		Oribacterium			
		Ornithobacterium			
		Oxalobacter			
		Peptoniphilus			
		Pimelobacter			
		Planktothrix			
		Porphyromonas			
		Prosthecobacter			
		Proteus			
		Pseudidiomarina			
		Pseudoramibacter_ Eubacterium			
		Ramlibacter			
		Reinekea			
		Robiginitalea			
		Roseburia			
		Roseomonas			
		Saccharothrix			
		Salinicoccus			
		Shewanella			
		Shinella			
		Sporosarcina			
		Sutterella			
		Syntrophomonas			
		Thalassospira			
		WAL_1855D			
		WCHB1-05			

Table 2 Microbial genera common to all the stages of spike development

Bacterial members	Fungal members
Achromobacter	*Acremonium*
Acinetobacter	*Acrocalymma*
Actinoplanes	*Alternaria*
Adhaeribacter	*Ascochyta*
Agrobacterium	*Aspergillus*
Agromyces	*Aureobasidium*
Alicyclobacillus	*Bartalinia*
Ammoniphilus	*Basidiobolus*
Anaerolinea	*Bipolaris*
Anaeromyxobacter	*Bullera*
Ardenscatena	*Candida*
Bacillus	*Cercospora*
Bacteroides	*Chaetomella*
Balneimonas	*Chaetomium*
Bdellovibrio	*Cladosporium*
Bifidobacterium	*Colletotrichum*
Blautia	*Coniella*
Bradyrhizobium	*Coniothyrium*
Brevibacillus	*Coprinellus*
Bulleidia	*Cryptococcus*
Caldilinea	*Curvularia*
Caloramator	*Cystobasidium*
Candidatus Solibacter	*Debaryomyces*
Catenibacterium	*Epicoccum*
Chloronema	*Eutypella*
Chryseobacterium	*Fusarium*
Clostridium	*Gibellulopsis*
Collinsella	*Gliocladiopsis*
Comamonas	*Gliomastix*
Coprococcus	*Hannaella*
Corynebacterium	*Lambertella*
Dactylosporangium	*Lophiostoma*
Desulfovibrio	*Madurella*
Devosia	*Malassezia*
Dialister	*Medicopsis*
Dysgonomonas	*Melanodothis*
Enterococcus	*Microascus*
Erwinia	*Microdochium*
Euzebya	*Monocillium*
Faecalibacterium	*Mortierella*
Fimbriimonas	*Mycosphaerella*
Flavisolibacter	*Myrothecium*
Flavobacterium	*Neopyrenochaeta*
Fusobacterium	*Nigrospora*
Gemmata	*Ophiocordyceps*
Gluconacetobacter	*Penicillium*
Haemophilus	*Peniophora*
Herbaspirillum	*Phaeosphaeria*
Hymenobacter	*Phoma*
Janthinobacterium	*Plectosphaera*
Kaistobacter	*Podosphaera*
Kineococcus	*Polypaecilum*
Klebsiella	*Pseudozyma*
Lactobacillus	*Pyrenochaeta*
Leptolyngbya	*Queiroziella*
Luteolibacter	*Rhodotorula*
Lysobacter	*Saccharomycopsis*
Marinobacter	*Sarocladium*
Megasphaera	*Sterigmatomyces*
Methanosaeta	*Strelitziana*
Methylobacterium	*Symmetrospora*
Methylophaga	*Taphrina*
	Torula
Mycobacterium	*Toxicocladosporium*
Nitrospira	*Trichoderma*
Nocardia	*Trichothecium*
Nocardioides	*Verticillium*
Opitutus	*Vishniacozyma*
Oscillochloris	*Volutella*
Oscillospira	*Wallemia*
Paenibacillus	
Parabacteroides	
Phascolarctobacterium	
Pirellula	
Planctomyces	
Prevotella	
Proteiniclasticum	
Pseudoalteromonas	
Pseudomonas	
Pseudonocardia	
Rhodococcus	
Rhodoplanes	
Rothia	
Rubrobacter	
Ruminococcus	
Salmonella	
Sedimentibacter	
Sediminibacterium	
Serratia	
Sphingomonas	
Staphylococcus	
Stenotrophomonas	
Steroidobacter	
Streptococcus	
Streptomyces	
Symbiobacterium	
T78	
Trabulsiella	
Treponema	
vadinCA02	
Virgisporangium	

Discussion

Recent studies on plant microbiomes have highlighted the previously neglected role of endophytic microbiota on plant health and productivity (Singh et al. 2022). It has been proposed that microbes, with their short life span, are more potent than plants in adapting to environmental factors or a particular niche. In addition, endophytes have been reported to produce a range of bioactive compounds, including plant metabolites such as taxol, camptothecin, hypericin, etc. (reviewed by Mishra et al. 2021c, 2022). Therefore, exploring the plant-associated microbiome for solving issues ranging from agricultural sustainability to bioprospecting is pertinent.

Despite the advancements in our understanding of the plant–microbe association, the effect of the developmental stage on the endophytic microbiome is poorly

understood. Here, we have investigated the diversity and abundance of bacterial and fungal communities during different stages of spike development in *P. longum*. The female spikes of *P. longum* are rich in pharmacologically important bioactive compounds, especially piperine and piperlongumine (Rajopadhye et al. 2012; Basak and Mohapatra 2015). In a previous study, we reported the endophytic bacterial and fungal communities associated with leaf and spike tissues of *P. longum* (Mishra et al. 2021b). The spikes were preferentially associated with microbial communities that have been reported to produce economically important secondary metabolites, including piperine. Therefore, we were interested in studying the microbiome associated with spikes, from the young to the mature phase. Spike samples representing three stages (early, mid, and late) of spike development were investigated by targeted amplicon sequencing of 16S rRNA gene and ITS region to determine changes, if any, in the abundance and composition of endophytic microbial communities during development. To rule out the interference of environmental and edaphic factors on microbial structure and composition, spikes borne on *P. longum* plants growing in the same geographical location, under the same environmental conditions were collected on the same day.

Spike development is marked by remarkable shifts in the microbiota

The 16S rRNA gene and ITS amplicon sequencing analysis clearly showed that the spike endosphere microbiota was not static; it underwent significant changes both in abundance and diversity at different stages of spike development. Further, while some microbial communities were exclusively or preferentially associated with certain developmental stages, others were present throughout spike development. However, it must be noted that even those present at all the stages or common microbiota underwent a striking change in their abundance level during spike development. Notably, the mid and late stages of spike development were accompanied by a more heterogeneous assemblage of bacterial communities encompassing members from various classes, namely *Gamma Proteobacteria, Clostridia, Anaerolineae, Actinobacteria* and *Bacilli*. The fungal communities belonging to *Ustilaginomycetes* and *Dithediomycetes* showed an increase in abundance, while those belonging to *Tremellomycetes*, *Saccharomycetes* and *Wallemiomycetes* decreased in abundance as the spike development progressed. These interesting trends in the relative abundance of these microbial taxa could indicate an underlying function; this remains a task for the future.

Interestingly, *Mortierella, Cladosporium* and *Basidiobolus* more or less remained the three most abundant fungal genera during spike development. Further, *Mortierella* and *Cladosporium* (along with *Vishniacozyma* and *Sphingomonas*) were also found to represent the core microbial communities of spikes. In a previous study, *M. alpina* CS10E4 has been reported to enhance the production of apocarotenoids, namely crocin, picrocrocin and safranal, improve growth parameters, and stress tolerance in *Crocus sativus* (Wani et al. 2017). Moreover, *M. elongata* strains isolated from *Populus* field sites have been found to improve plant biomass in various crop species, including *Populus, Citrullus lanatus, Zea mays, Solanum lycopersicum,* and *Cucurbita* (Zhang et al. 2020). *Cladosporium* is another core endophytic fungus of *P. longum* spikes. Previous reports have demonstrated the ability of endophytic *Cladosporium* strains to produce bioactive compounds such as polyketides from a *Cladosporium* strain isolated from *Excoecaria agallocha* (Wang et al. 2018), and Huperzine A, which is used in the treatment of Alzheimer's disease (Zhang et al. 2011). Further, *Cladosporium*-mediated synthesis of silver nanoparticles has been found to have antioxidant, anti-diabetic and anti-Alzheimer activity (Popli et al. 2018). Endophytic strains of *Sphingomonas* have been reported to demonstrate plant growth promoting properties, including the production of IAA and gibberellins (Khan et al. 2014) and alleviation of heavy metal stresses (Bilal et al. 2018; Wang et al. 2020). The other abundant genus in spikes, *Herbaspirillum*, has been reported to occur as diazotrophic bacterial endophyte in various Gramineae members (Olivares et al. 1996; Pedrosa et al. 2011).

Since all the spike samples were collected from the plants (*P. longum* plants show staggered flowering pattern), growing in the same area and at the same time, the underlying cause for the change in spike-associated microbiota is most likely development-specific. Besides, the stage-specific association or dynamics of spike-associated microbiota could be explained by two possibilities: either the host (plant) genotype actively recruits or increases the titre of some members at a specific stage of spike development, or the microbial communities regulate their number in response to metabolites or factors present at specific stages of development.

Identification of biomarkers, core and stage-specific microbiota

The occurrence of microbial taxa across different samples could be used as a parameter to determine the core microbial communities (Neu et al. 2021). In the present study, *Sphingomonas, Mortierella, Cladosporium* and *Vishniacozyma* represented the core microbiota of spikes; these were shared among all the spike development stages at significant cut-off values. It could be inferred that core endophyte communities

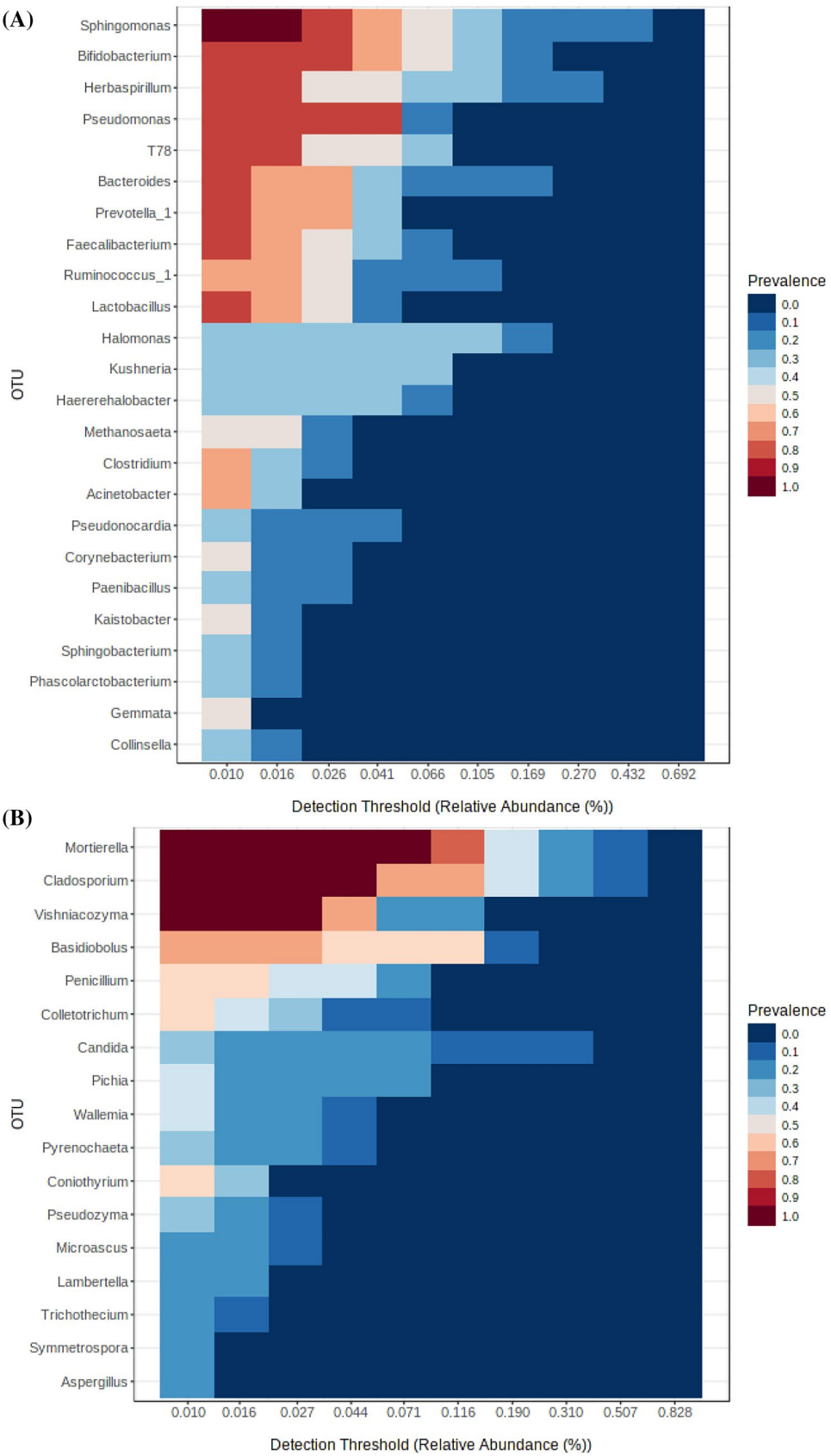

Fig. 5 Core microbiome of spike-associated bacterial (**A**) and fungal (**B**) communities. The data was visualized with the sample prevalence of 20% and relative abundance of 0.1%

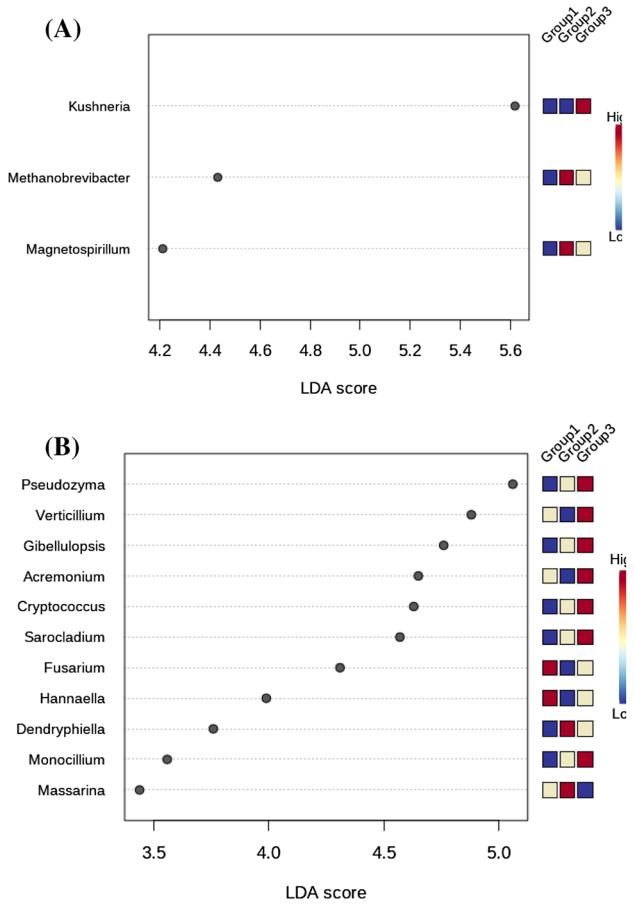

Fig. 6 LEfSe analysis of bacterial (**A**) and fungal (**B**) OTUs at genus level for biomarker discovery. Group I represents early stage (SI); Group II indicates mid stage (SII) and Group III indicates late stage (SIII) of spike development

would have evolved to stably colonize the particular niche (plant endosphere), and have most likely developed an intricate functional or physiological association with the host. The knowledge of core microbiota would enable targeted culturing protocols for isolating and characterizing the core microbial communities. The investigation of the core microbiome would provide crucial insights into the *in planta* function of these microbial communities. Often considered as obligate partners of the host, core microbiome could also be defined and delineated based on the "ecological core", "functional core" or "temporal core" (Neu et al. 2021).

Next, three derived analyses, namely Linear Discriminant Analysis (LDA) Effect Size (LEfSe), correlation network analysis, and PICRUSt and functional guild analysis, were performed to gain clues on the functional role(s) of spike-associated microbiome. LEfSe analysis was performed to determine the OTUs/microbial taxa that would explain the differences observed between different stages of spike development. In other words, the bacterial and fungal communities that could be used as biomarkers for particular stages of spike development have been identified based on changes in abundance. Based on the results of LEfSe analysis, it could be inferred that *Kushneria* was highly abundant at the SIII stage, while *Methanobrevibacter* and *Magnetospirillum* were at the SII stage (Fig. 6A). Likewise, the corresponding fungal biomarkers for the SIII stage were *Pseudozyma, Verticillium, Gibellulopsis, Acremonium, Cryptococcus* and *Sarocladium* (Fig. 6B).

The results of the co-relation analysis revealed co-occurrence and interdependence of microbial communities at particular stages. Besides, correlation analysis may indicate ecological interactions between microbial communities. Our results indicated that the abundance of *Sphingomonas* during spike development was negatively co-related with that of *SHD_231* (Fig. 7A and 3B). Interestingly, the correlation analysis performed for fungal communities revealed a highly intricate association among the fungal taxa than the bacterial ones. The significant co-occurrence of microbial communities at a particular stage of spike development indicates a similar niche, and could imply interdependence, teamwork or division of labor for a particular plant response or simply similar physiological requirements of the microbiota.

Metabolic potential and trophic mode analysis of spike-associated microbiota during spike development

The potential metabolic functions of bacterial communities during spike development were predicted by PICRUSt analysis. The results indicated that amino acid biosynthesis and metabolism was the predominant function performed by spike-associated bacteriome (Fig. 8). The other major functions attributed to spike-inhabiting microbial communities included metabolism of nitrogen, nucleic acids and carbohydrates. Further, there was some representation of microbiome-specific carbon fixation in the spike-associated bacterial communities. Overall most biological functions were slightly over-represented during the SIII spike development stage. The category of "amino sugar and nucleotide sugar metabolism" was exclusively represented in the bacterial communities present during the late spike development stage. Likewise, "nicotinate and nicotinamide metabolism" was represented in spike-associated bacteria during the mid- and late-spike development stages (Fig. 8).

Next, the FUNGuild analysis was performed to predict the tropic modes (Fig. 9A) and functional guilds (Fig. 9B) of the spike-associated fungal communities during spike development (Nguyen et al. 2016). The results suggested that the proportion of fungal communities with "pathotroph" and "pathotroph-symbiotroph" mode increased during spike

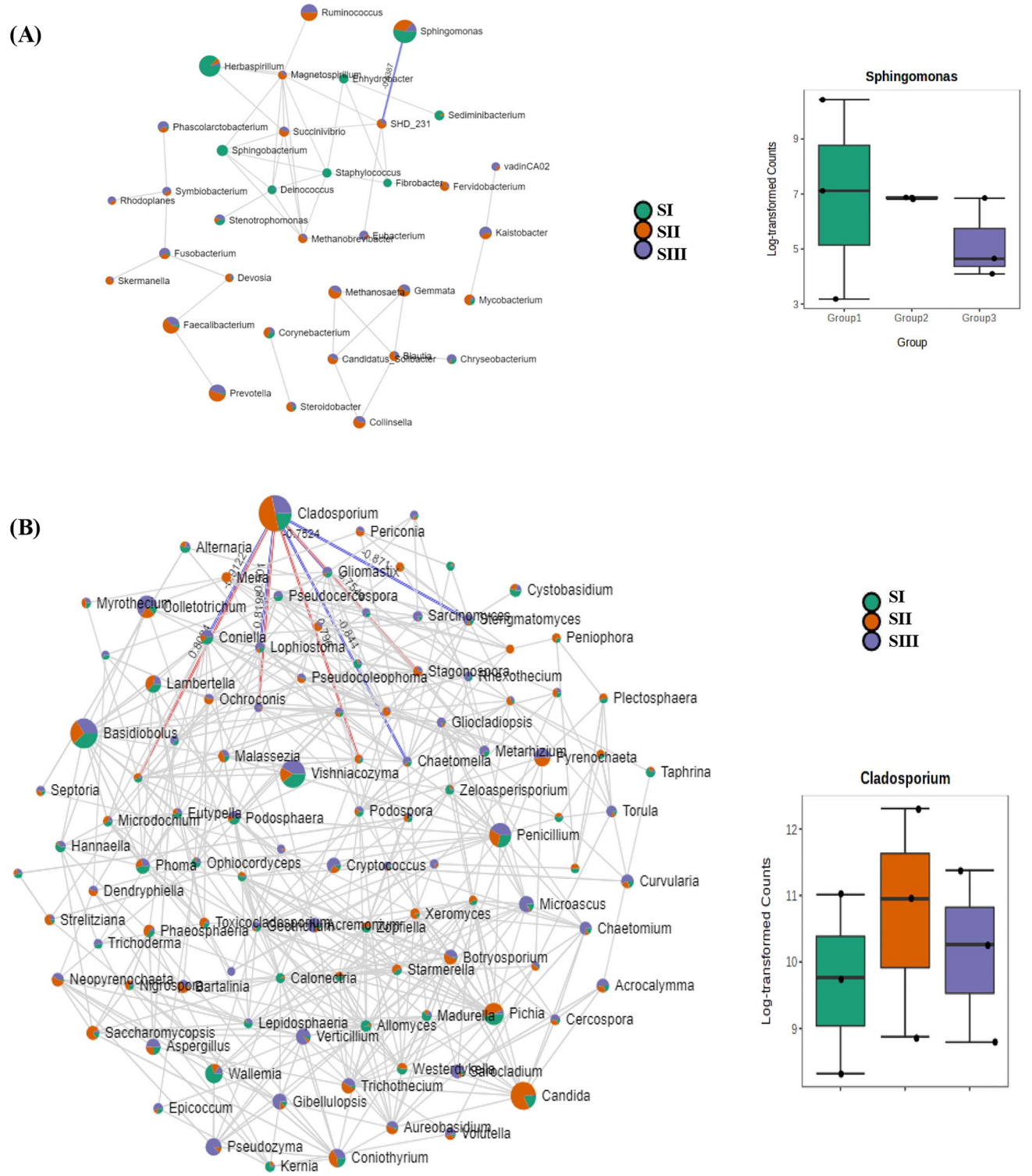

Fig. 7 Correlation network for bacterial (**A**) and fungal (**B**) genera during early (SI), mid (SII) and late (SIII) stages of spike development. Links between nodes are based on correlations and represent potential interaction(s) among taxa

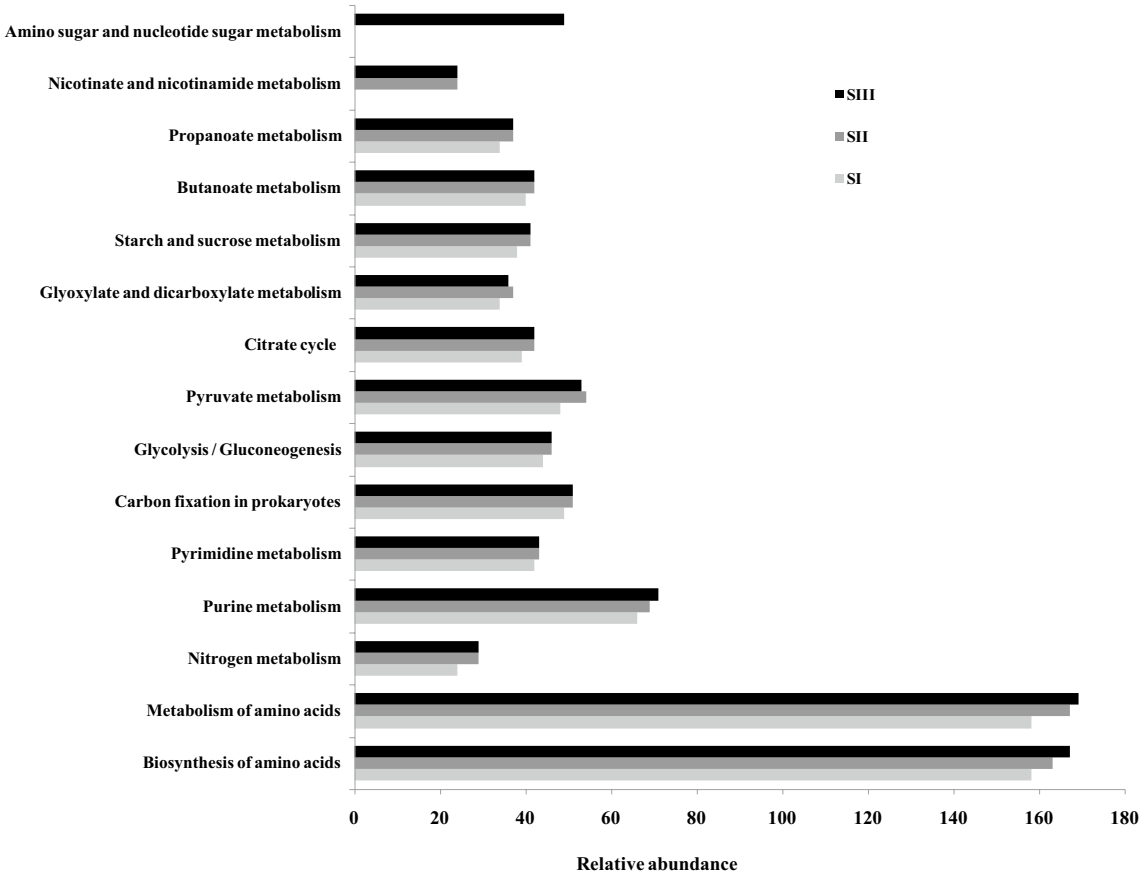

Fig. 8 Prediction of metabolic functions of bacterial communities by PICRUSt analysis. Bar plots display the mean proportion for each of the 15 KEGG pathways that were found to be different in spike-associated bacterial communities during spike development. SI, SII, and SIII represent early, mid, and late stages of development, respectively

development. Further, the "endophyte-plant pathogen" guild was over-represented in the fungal taxa associated with the later stages of spike development.

Conclusions

The microbiome constitutes a significant part of the holobiont, and is often considered the "second genome" of an organism. Although the role of plant microbiome in plant health and stress responses is beginning to get attention, its role or abundance *vis-a-vis* plant development is largely unexplored. This is the first report to investigate the temporal association of endophyte communities in response to spike (fruit) development. Our results indicate that the spike development in *P. longum* is accompanied by a remarkable shift in microbiota. This transition is especially prominent during the later stages of spike development, which overlaps with the mature, dark-green stage or the "*pippali*" of commerce. Considering the economic importance of piperine and other spike-derived alkaloids, understanding the composition and abundance of microbial communities in spikes and their dynamics as a function of development, is the key to bioprospecting for economically important metabolites. Based on the results of targeted metagenomic analysis, concerted efforts should be made to isolate and culture promising strains in laboratory. This, followed by designing a synthetic microbial community of selected bacterial and fungal isolates, could act as an in vitro model system wherein factors such as temperature, pH, culture media etc. could be altered, and inducers/inhibitors could be added to investigate their effect on the production of important metabolites. Apart

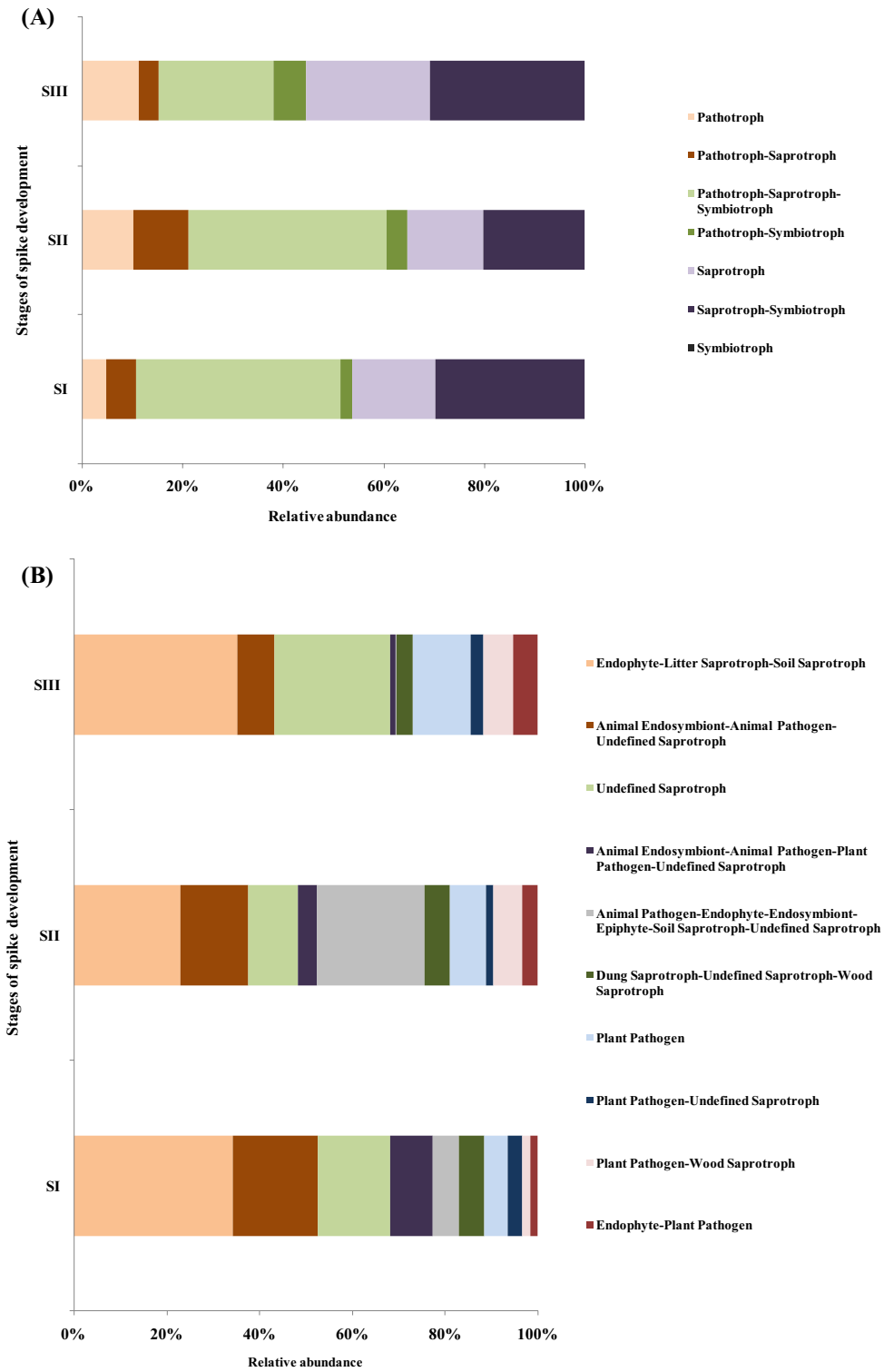

Fig. 9 Stacked bar plots representing the trophic modes (**A**), and top ten guilds (**B**) of fungal communities associated with spikes during early (SI), mid (SII) and late (SIII) stages of spike development. The trophic modes and guilds were predicted by FUNGuild analysis

from bioprospecting for economically significant plant metabolites, the findings of the present study could be pursued for their potential applications in biotechnology, agriculture, medicine and environment.

Supplementary Information The online version contains supplementary material available at https://doi.org/10.1007/s12298-023-01352-2.

Acknowledgements SM and SS are grateful to the Science and Engineering Research Board-Teachers Associateship for Research Excellence (SERB-TARE) for research grant TAR/2021/000309.

Author contributions SM and SS conceptualized the research design and procured funding; SM performed the experiments and data analysis; SM wrote the manuscript; SS provided critical inputs and reviewed the manuscript. Both authors have read and approved the submitted manuscript.

Availability of data and material The 16S rRNA gene and ITS sequencing reads have been deposited in the Sequence Read Archive of the National Centre for Biotechnology Information under the Bioproject number, PRJNA860932 and PRJNA869034, respectively.

Declarations

Conflict of interest The authors declare no conflict of interest.

References

Atal N, Bedi KL (2010) Bioenhancers: revolutionary concept to market. J Ayurveda Integr Med 1(2):96–99

Babu KN, Divakaran M, Ravindran PN, Peter KV (2006) Long pepper. In: Peter KV (ed) Handbook of herbs and spices. Woodhead Publishing, Sawston, pp 420–437

Basak UC, Mohapatra M (2015) Comparative appraisal of piperine content in various female spikes of *Piper longum* Linn., a RET medicinal plant of Odisha. World J Pharma Res 4(11):1048–1058

Bilal S, Shahzad R, Khan AL, Kang SM, Imran QM, Al-Harrasi A, Yun BW, Lee IJ (2018) Endophytic microbial consortia of phytohormones-producing fungus Paecilomyces formosus LHL10 and bacteria *Sphingomonas* sp. LK11 to *Glycine max* L. regulates physio-hormonal changes to attenuate aluminum and zinc stresses. Front Plant Sci 9:1273

Bolyen E, Rideout JR, Dillon MR, Bokulich NA, Abnet CC, Al-Ghalith GA, Alexander H, Alm EJ, Arumugam M, Asnicar F, Bai Y (2019) Reproducible, interactive, scalable and extensible microbiome data science using QIIME 2. Nat Biotechnol 37(8):852–857

Chaparro JM, Badri DV, Vivanco JM (2014) Rhizosphere microbiome assemblage is affected by plant development. ISME J 8(4):790–803

Gajurel PR, Kashung S, Nopi S, Panmei R, Singh B (2021) Can the Ayurvedic pippali plant (*Piper longum* L.) be a good option for livelihood and socio-economic development for Indian farmers? Curr Sci 120(10):1567–1572

Houlden A, Timms-Wilson TM, Day MJ, Bailey MJ (2008) Influence of plant developmental stage on microbial community structure and activity in the rhizosphere of three field crops. FEMS Microbiol Ecol 65(2):193–201

Joshi K, Panara K, Nishteswar K, Chaudhary S (2013) Cultivation and pharmacological profiles of root of *Piper longum* Linn. Pharma Sci Monit 4(1):3617–3627

Kanimozhi K, Sujatha VS (2016) Reproductive biology of *Piper longum* L. J Trop Agric 53(2):206–212

Khan AL, Waqas M, Kang SM, Al-Harrasi A, Hussain J, Al-Rawahi A, Al-Khiziri S, Ullah I, Ali L, Jung HY, Lee IJ (2014) Bacterial endophyte *Sphingomonas* sp. LK11 produces gibberellins and IAA and promotes tomato plant growth. J Microbiol 52(8):689–695

Khound A, Sharmah D, Barua PC (2019) Variation in spike initiation in some *Piper longum* germplasms of North East India. J Appl Nat Sci 11(3):684–686

Klindworth A, Pruesse E, Schweer T, Peplies J, Quast C, Horn M, Glöckner FO (2013) Evaluation of general 16S ribosomal RNA gene PCR primers for classical and next-generation sequencing-based diversity studies. Nucleic Acids Res 41(1):e1. https://doi.org/10.1093/nar/gks808

Langille MG, Zaneveld J, Caporaso JG, McDonald D, Knights D, Reyes JA, Clemente JC, Burkepile DE, Vega Thurber RL, Knight R, Beiko RG (2013) Predictive functional profiling of microbial communities using 16S rRNA marker gene sequences. Nat Biotechnol 31(9):814–821

Mintoo MN, Mishra S, Dantu PK (2019) Isolation and characterization of endophytic bacteria from *Piper longum*. Proc Nat Acad Sci, India Sect b: Biol Sci 89(4):1447–1454

Mishra S, Bhattacharjee A, Sharma S (2021a) An ecological insight into the multifaceted world of plant-endophyte association. Crit Rev Plant Sci 40(2):127–146

Mishra S, Goyal D, Phurailatpam L (2021b) Targeted 16S rRNA gene and ITS2 amplicon sequencing of leaf and spike tissues of *Piper longum* identifies new candidates for bioprospecting of bioactive compounds. Arch Microbiol 203(7):3851–3867

Mishra S, Sahu PK, Agarwal V, Singh N (2021c) Exploiting endophytic microbes as micro-factories for plant secondary metabolite production. Applied Microbiol Biotechnol 105(18):6579–6596

Mishra S, Bhardwaj P, Sharma S (2022) Metabolomic insights into endophyte-derived bioactive compounds. Front Microbiol 13:835931. https://doi.org/10.3389/fmicb.2022.835931

Neu AT, Allen EE, Roy K (2021) Defining and quantifying the core microbiome: challenges and prospects. Proc NatAcad Sci 118(51):e2104429118

Nguyen NH, Song Z, Bates ST, Branco S, Tedersoo L, Menke J, Schilling JS, Kennedy PG (2016) FUNGuild: an open annotation tool for parsing fungal community datasets by ecological guild. Fungal Ecol 20:241–248

Olivares FL, Baldani VL, Reis VM, Baldani JI, Döbereiner J (1996) Occurrence of the endophytic diazotrophs *Herbaspirillum* spp. in roots, stems, and leaves, predominantly of Gramineae. Biol Fert Soils 21(3):197–200

Pedrosa FO, Monteiro RA, Wassem R, Cruz LM, Ayub RA, Colauto NB, Fernandez MA, Fungaro MHP, Grisard EC, Hungria M, Madeira HM (2011) Genome of *Herbaspirillum seropedicae* strain SmR1, a specialized diazotrophic endophyte of tropical grasses. PLoS Genet 7(5):e1002064

Phurailatpam L, Gupta A, Sahu PK, Mishra S (2022) Insights into the functional potential of bacterial endophytes from the ethnomedicinal plant *Piper Longum* L. Symbiosis 87(2):165–174

Popli D, Anil V, Subramanyam AB, Namratha MN, Ranjitha VR, Rao SN, Rai RV, Govindappa M (2018) Endophyte fungi, *Cladosporium* species-mediated synthesis of silver nanoparticles possessing in vitro antioxidant, anti-diabetic and anti-Alzheimer activity. Artif Cells Nanomed Biotechnol 46(sup1):676–683

Rajopadhye AA, Namjoshi TP, Upadhye AS (2012) Rapid validated HPTLC method for estimation of piperine and piperlongumine in root of *Piper longum* extract and its commercial formulation. Rev Bras 22:1355–1361

Singh A, Hidangmayum A, Yashu BR, Kumar V, Singh BN, Dwivedi P (2022) Underlying forces of plant microbiome and their effect on plant development. In: Singh HB, Vaishnav A (eds) New and future developments in microbial biotechnology and bioengineering. Elsevier, New York

Ved DK and Goraya GS (2008) A text book of demand and supply of medicinal plants in India. NMPB, New Delhi and FRLHT, Bangalore, India

Vikaspedia: https://vikaspedia.in/agriculture/crop-production/package-of-practices/medicinal-andromatic-plants/piper-longum

Wang H, Yang J, Zhou L, Luo B, Cheng X, Zhang C, Tang X, Pan L, Liu L, Yang Q (2019) Chemical compositions and pharmacological activities of *Polygoni multiflori* radix. Chin J Exp Tradit Med Formulae 24(13):192–205

Wang Q, Ge C, Xu SA, WuY SZA, Ma L, Pan F, Zhou Q, Huang L, Feng Y, Yang X (2020) The endophytic bacterium *Sphingomonas* SaMR12 alleviates Cd stress in oilseed rape through regulation of the GSH-AsA cycle and antioxidative enzymes. BMC PlantBiol 20(1):1–14

Wang L, Han X, Zhu G, Wang Y, Chairoungdua A, Piyachaturawat P, Zhu W (2018) Polyketides from the endophytic fungus *Cladosporium* sp. isolated from the mangrove plant Excoecaria agallocha. Front Chem 6:344

Wani ZA, Kumar A, Sultan P, Bindu K, Riyaz-Ul-Hassan S, Ashraf N (2017) Mortierella alpina CS10E4, an oleaginous fungal endophyte of *Crocus sativus* L. enhances apocarotenoid biosynthesis and stress tolerance in the host plant. Sci Rep 7(1):1–11

White TJ, Bruns T, Lee SJWT, Taylor J (1990) Amplification and direct sequencing of fungal ribosomal RNA genes for phylogenetics. PCR Protoc Guide Methods Appl 18(1):315–322

Zhang ZB, Zeng QG, Yan RM, Wang Y, Zou ZR, Zhu D (2011) Endophytic fungus *Cladosporium cladosporioides* LF70 from *Huperzia serrata* produces Huperzine A. World J Microbiol Biotechnol 27(3):479–486

Zhang K, Bonito G, Hsu CM, Hameed K, Vilgalys R, Liao HL (2020) *Mortierella elongata* increases plant biomass among non-leguminous crop species. Agronomy 10(5):754